iScience

CellPress
OPEN ACCESS

Article

6-Thioguanine blocks SARS-CoV-2 replication by inhibition of PLpro

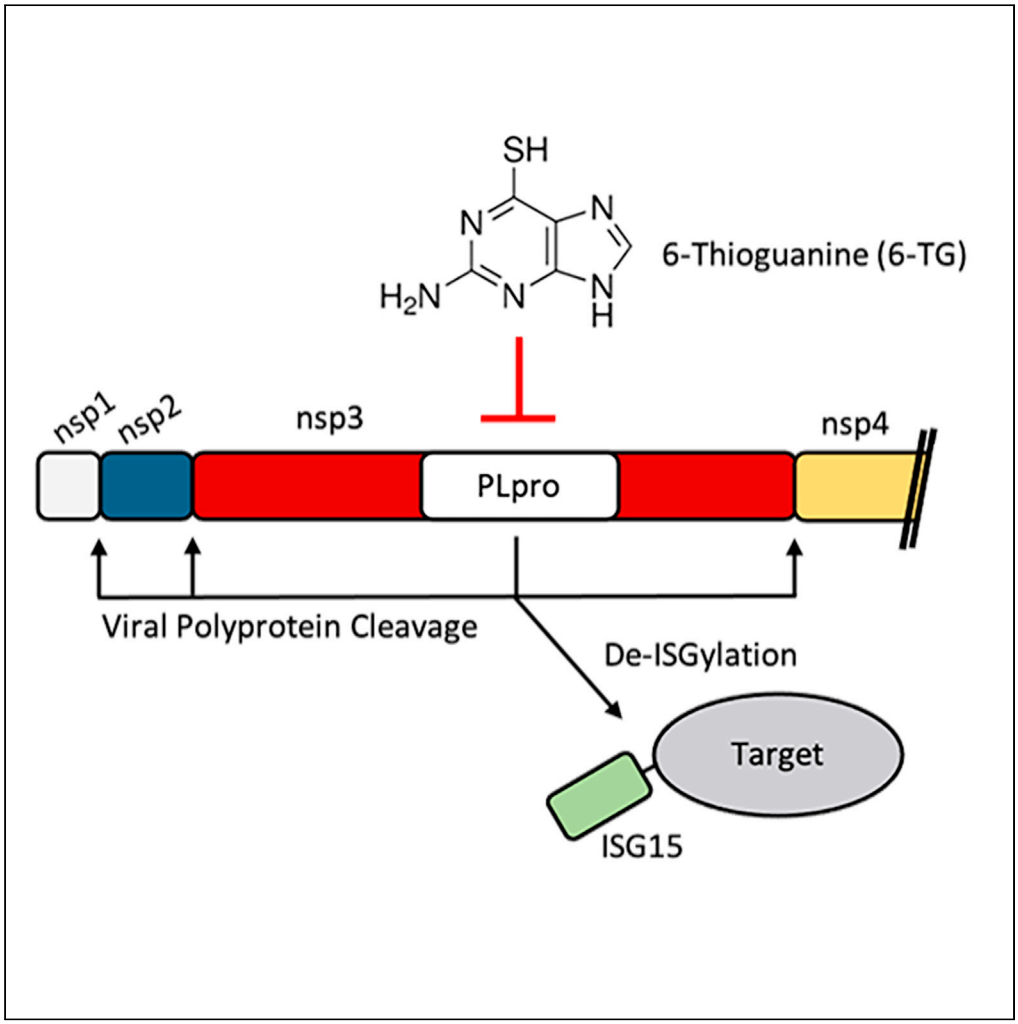

Caleb D. Swaim, Varun Dwivedi, Yi-Chieh Perng, ..., Deborah J. Lenschow, Viraj Kulkarni, Jon M. Huibregtse

huibregtse@austin.utexas.edu

Highlights

6-Thioguanine (6-TG) is a direct-acting antiviral against SARS-CoV-2

6-TG targets the papain-like protease (PLpro) activity of the viral nsp3 protein

6-TG is a well-characterized and inexpensive orally-delivered drug

6-TG is a potentially useful therapeutic for COVID-19

Swaim et al., iScience *24*, 103213
October 22, 2021
https://doi.org/10.1016/j.isci.2021.103213

iScience

CellPress
OPEN ACCESS

Article

6-Thioguanine blocks SARS-CoV-2 replication by inhibition of PLpro

Caleb D. Swaim,[1] Varun Dwivedi,[2] Yi-Chieh Perng,[3] Xu Zhao,[1] Larissa A. Canadeo,[1] Houda H. Harastani,[3] Tamarand L. Darling,[3] Adrianus C.M. Boon,[3,4,5] Deborah J. Lenschow,[3,4] Viraj Kulkarni,[2] and Jon M. Huibregtse[1,6,*]

SUMMARY

The emergence of SARS-CoV-2 has led to a global health crisis that, in addition to vaccines and immunomodulatory therapies, calls for the identification of antiviral therapeutics. The papain-like protease (PLpro) activity of nsp3 is an attractive drug target as it is essential for viral polyprotein cleavage and for deconjugation of ISG15, an antiviral ubiquitin-like protein. We show here that 6-Thioguanine (6-TG), an orally available and widely available generic drug, inhibits SARS-CoV-2 replication in Vero-E6 cells with an EC50 of approximately 2 μM. 6-TG also inhibited PLpro-catalyzed polyprotein cleavage and de-ISGylation in cells and inhibited proteolytic activity of the purified PLpro domain *in vitro*. We therefore propose that 6-TG is a direct-acting antiviral that could potentially be repurposed and incorporated into the set of treatment and prevention options for COVID-19.

INTRODUCTION

Coronavirus Disease-2019 (COVID-19) is caused by SARS-CoV-2, a betacoronavirus highly similar to SARS-CoV-1 (now SARS-CoV-1) (Coronaviridae Study Group of the International Committee on Taxonomy of Viruses, 2020; Gralinski and Menachery, 2020). An urgent need exists for additional treatment strategies, and repurposed FDA-approved drugs with existing supply chains and well characterized pharmacologic properties represent a rapid and efficient approach toward COVID-19 therapeutics (Guy et al., 2020).

Enzymatic activities encoded by SARS-CoV-2 are attractive drug targets, including PLpro, an essential cysteine protease within the large multi-domain nsp3 protein (Harcourt et al., 2004). PLpro cleaves the pp1a polyprotein at three sites and is required to generate the mature nsp1, 2, 3 and 4 proteins. These proteins modulate host cell translation (nsp1) and contribute to formation of viral replication/transcription complexes (nsp2, 3, and 4) (V'kovski et al., 2021). The PLpro recognition consensus site within pp1a (LXGG) is also found at the C-terminus of ubiquitin and ISG15, an antiviral ubiquitin-like modifier, although PLpro of MERS-CoV, SARS-CoV-1, and SARS-CoV-2 PLpro preferentially catalyzes de-ISGylation over ubiquitylation (Daczkowski et al., 2017; Freitas et al., 2020). The fact that these viruses encode de-ISGylase activity suggests they are sensitive to the antiviral effects of ISGylation. Therapeutic inhibition of PLpro would therefore be predicted to have two antiviral effects: inhibition of viral replication by blocking polyprotein cleavage and restoration of the antiviral effects of ISGylation. Further, de-ISGylation by PLpro, through generation of free (unconjugated) ISG15, enhances the secretion and extracellular signaling function of ISG15, which in turn promotes pro-inflammatory cytokine production from cells of the immune system (Swaim et al., 2020). Therefore, a potential third effect of inhibiting PLpro would be a decrease in the pro-inflammatory "cytokine storm" associated with COVID-19 (Tay et al., 2020). Here, we show that an inhibitor of SARS-CoV-2 PLpro, 6-thioguanine (6-TG), inhibits virus replication at low micromolar concentrations. 6-TG is a widely available generic drug that could therefore potentially be repurposed as a betacoronavirus therapeutic in the current and future pandemics.

RESULTS

6-Thioguanine inhibits SARS-CoV-2 replication

6-Thioguanine (Figure 1A) has been used clinically since the 1950s, originally for the treatment of childhood leukemias and subsequently for long-term treatment of inflammatory bowel disease (IBD) and Crohn's disease (Bayoumy et al., 2020). 6-TG was previously reported to inhibit the SARS-CoV-1 and MERS-CoV PLpro

[1]Department of Molecular Biosciences, University of Texas at Austin, Austin, TX, USA

[2]Disease Intervention and Prevention, Texas Biomedical Research Institute, San Antonio, TX, USA

[3]Department of Internal Medicine, Washington University School of Medicine, St. Louis, MO, USA

[4]Department of Pathology and Immunology, Washington University School of Medicine, St. Louis, MO, USA

[5]Department of Molecular Microbiology, Washington University School of Medicine, St. Louis, MO, USA

[6]Lead contact

*Correspondence: huibregtse@austin.utexas.edu

https://doi.org/10.1016/j.isci.2021.103213

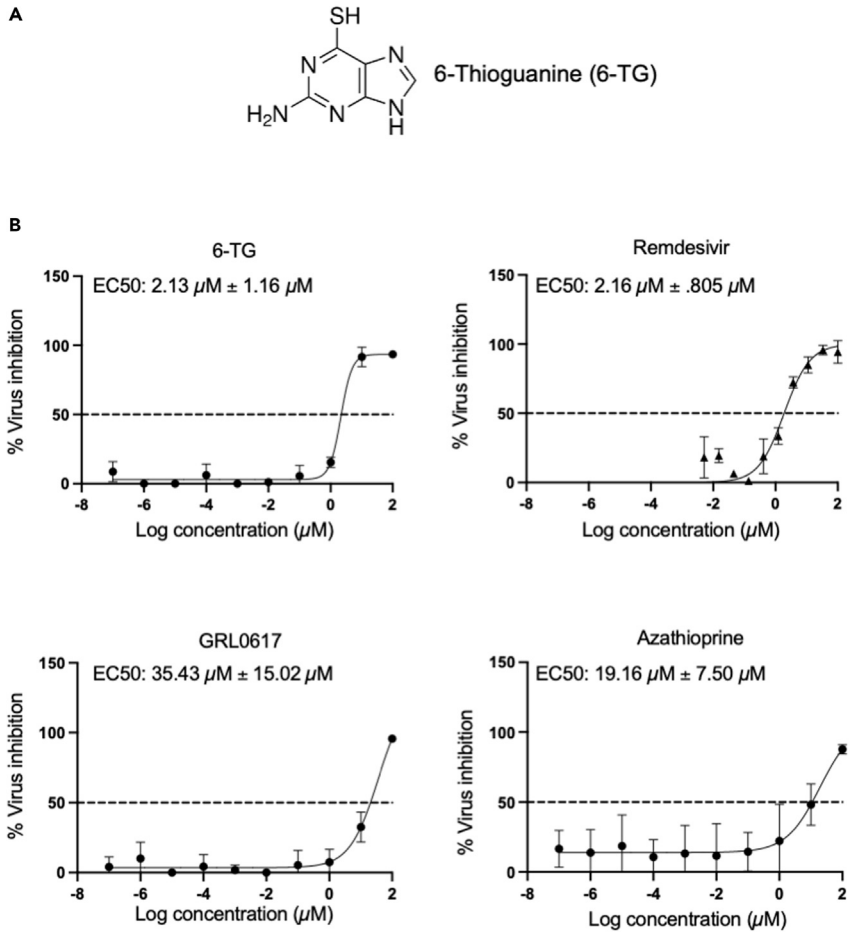

Figure 1. 6-TG inhibits SARS-CoV-2 viral replication in Vero-E6 cells

(A) The structure of 6-Thioguanine (6-TG).

(B) Vero-E6 cells were treated with 6-TG, Remdesivir, GRL0617, and Azathioprine to assess their ability to restrict SARS-CoV-2 replication (MOI: 0.01). Drug concentrations for 6-TG, GRL0617 and Azathioprine ranged from 0.1 pM to 100 μM at 10-fold increments; concentrations for Remdesivir ranged from 5 nM to 100 μM at 3-fold increments. Percent inhibition of viral replication was calculated by comparing plaques in drug-treated samples to those in DMSO treated samples and shown as mean ± SED for either four replicates (6-TG, GRL0617 and Azathioprine) or two replicates (Remdesivir). The calculated EC50 for the compounds are shown in each panel with 95% confidence limits.

catalytic domain *in vitro* (Cheng et al., 2015; Chou et al., 2008); however, there was no further follow up of its ability to inhibit de-ISGylation or viral polyprotein cleavage in cells or its ability to inhibit viral replication. 6-TG was therefore tested for its ability to inhibit SARS-CoV-2 replication in Vero-E6 African Green Monkey kidney cells. As shown in Figure 1B, 6-TG inhibited viral replication with a half-maximal effective concentration (EC50) of 2.13 μM. Remdesivir, a SARS-CoV-2 therapeutic and an inhibitor of the viral RNA-dependent RNA polymerase (Yin et al., 2020), inhibited replication with a very similar EC50, 2.16 μM. GRL0617, a previously reported inhibitor of SARS-CoV-2 PLpro inhibited replication with an EC50 approximately 15-fold higher than 6-TG (35.43 μM), consistent with previously reported results (Freitas et al., 2020). Azathioprine, a thiopurine related to 6-TG that is also used clinically for IBD (Bayoumy et al., 2020), was approximately 10-fold less effective at inhibiting viral replication than 6-TG (EC50 19.16 μM). The cytotoxicity of these compounds was determined, and the CC50 (50% cytotoxic concentration) ranged from approximately 35 μM for 6-TG to 60 μM for Remdesivir (Figure S1).

6-Thioguanine inhibits PLpro activity in cells and *in vitro*

An essential role of the PLpro domain of nsp3 is to generate the mature nsp1-4 proteins from the pp1a polyprotein through self-catalyzed cleavage reactions. To determine if 6-TG inhibited polyprotein cleavage

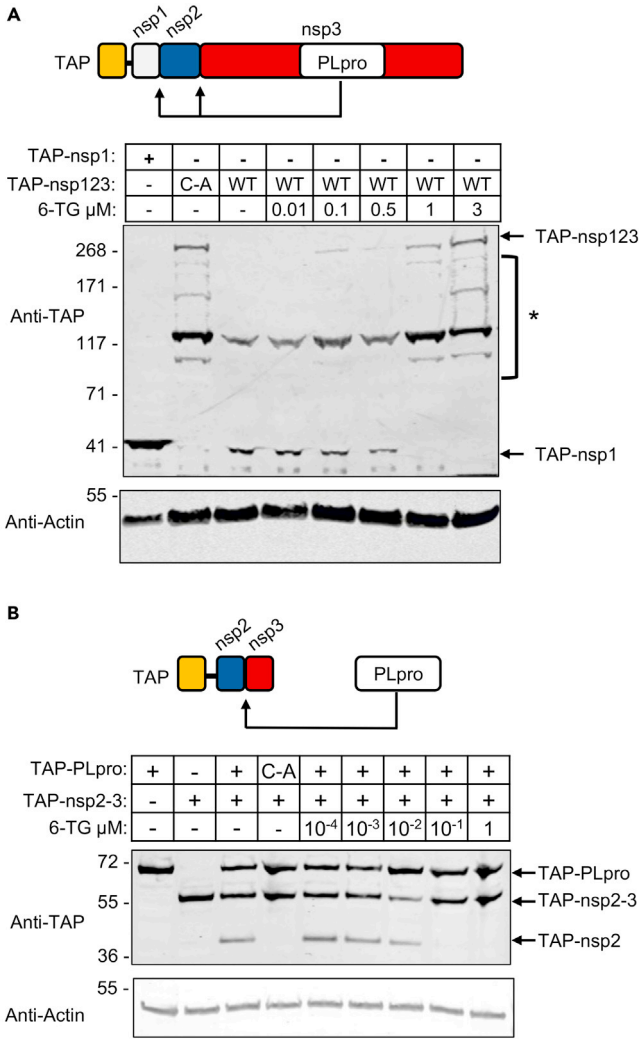

Figure 2. 6-TG inhibits viral polyprotein cleavage

(A) (Top) Schematic representation of the TAP-nsp123 fusion protein. Arrows indicate sites of PLpro-catalyzed cleavage. (Bottom) HEK293T cells were transfected with plasmids expressing either TAP-nsp1, TAP-nsp123^{WT} or TAP-nsp123^{CA}. 6-TG was added at the time of plasmid transfection and at the indicated final concentrations. Total cell lysates were prepared 48 h post-transfection and analyzed by immunoblotting with anti-TAP antibody. Bands corresponding to TAP-nsp1 and the full-length fusion proteins are indicated. Bracketed bands (*) represent breakdown products of the full-length WT or CA fusion proteins.

(B) (Top) Schematic representation of the TAP-nsp2-3 fusion protein. Arrow indicates site of PLpro-catalyzed cleavage. (Bottom) HEK293T cells were transfected with plasmids expressing TAP-nps2-3, and TAP-PLpro (WT or CA) and treated with 6-TG at the indicated final concentrations for 48 h. Total cell cell lysates were analyzed by TAP immunoblot. Bands corresponding to TAP-PLpro, TAP-nsp2-3 and TAP-nsp2 are indicated.

events in HEK293T cells, we expressed by plasmid transfection an N-terminally TAP-tagged pp1a protein consisting of the full-length nsp1, 2 and 3 proteins (TAP-nsp123^{WT}; Figure 2A). We also expressed a version of the protein with the active-site cysteine within the PLpro domain of nsp3 altered to an alanine (TAP-nsp123^{C-A}). The fusion proteins were detected by immunoblotting of cell lysates with anti-TAP antibody, and TAP-nsp1 was expressed separately as a size marker for the processed fusion protein. Expression of TAP-nsp123^{WT} resulted primarily in a product the size of TAP-nsp1 (42 kD), as expected if the fusion protein was fully processed, whereas expression of TAP-nsp123^{C-A} resulted in the expected full-length protein (336 kD) along with several breakdown products of the full-length protein. Increasing concentrations of 6-TG inhibited PLpro-mediated processing of the TAP-nsp123^{WT} polyprotein, with loss of the TAP-nsp1 product and accumulation of the full-length fusion protein, with the same pattern of breakdown products

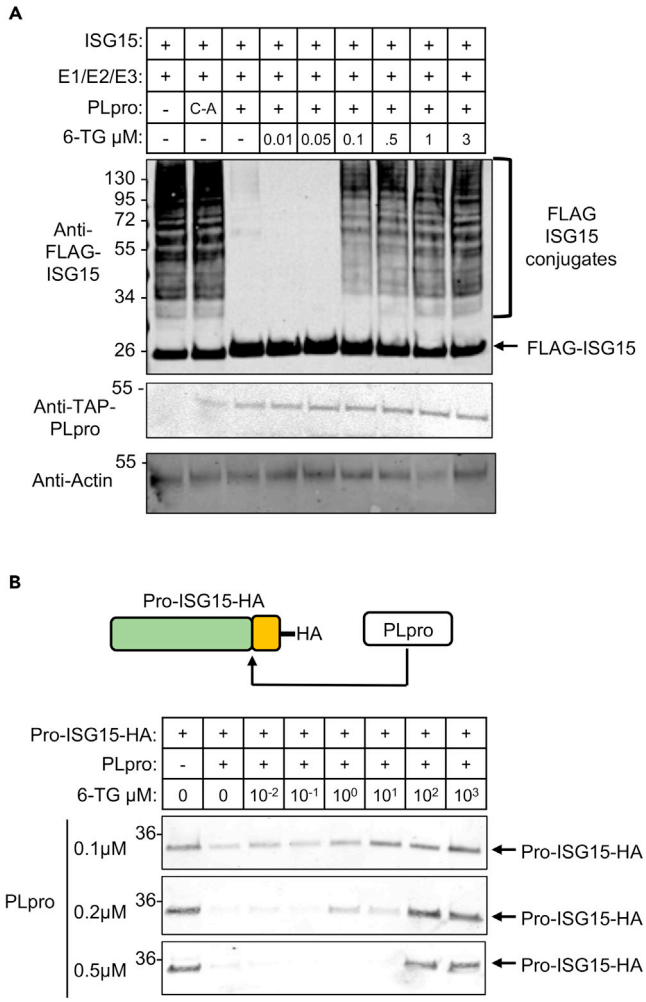

Figure 3. 6-TG inhibits PLpro-mediated de-ISGylation in cells and *in vitro*

(A) HEK293T cells were transfected with plasmids expressing FLAG-ISG15 and the ISG15 E1/E2/E3 enzymes and 0.2 μg of PLpro plasmid (WT or CA) where indicated. 6-TG was added at the time of transfection and at the indicated final concentrations. Total cell lysates were prepared 48 h post-transfection and analyzed by immunoblotting to detect FLAG-ISG15 and FLAG-ISG15 conjugates.

(B) (Top) Schematic of Pro-ISG15-HA where the mature ISG15 protein sequence (green) is expressed with its natural C-terminal extension (yellow), followed by an HA epitope tag. (Bottom) Purified Pro-ISG15-HA protein (100 ng) was incubated with the indicated concentrations of PLpro and 6-TG for 30 min and analyzed by HA immunoblot.

seen with the TAP-nsp123^{C-A} protein (Figure 2A). Half-maximal inhibition of polyprotein cleavage occurred at approximately 0.5 μM 6-TG (quantitation shown in Figure S2A). In a related experiment (Figure 2B), the isolated PLpro domain (residues 746-1061 of nsp3) was co-expressed in *trans* with a TAP-tagged nsp2-nsp3 fragment (residues 727-918 of pp1a), spanning the nsp2-3 PLpro cleavage site. PLpro efficiently processed the TAP-nsp2-3 protein, dependent on the active-site cysteine, and this was again inhibited with increasing amounts of 6-TG, with half-maximal inhibition at approximately 1.0 μM 6-TG (quantitation shown in Figure S2B).

In addition to polyprotein cleavage activity, SARS-CoV-2 PLpro deconjugates ISG15 from proteins that have been modified by this antiviral ubiquitin-like protein (Klemm et al., 2020; Shin et al., 2020; Swaim et al., 2020). The E1, E2, and E3 enzymes for conjugation of human ISG15 are Uba7, Ube2L6, and Herc5, respectively, and expression of these enzymes with ISG15 results in robust protein ISGylation in cells (Dastur et al., 2006). Figure 3A shows that co-expression of PLpro (residues 746-1061 of nsp3) with ISG15 and the ISG15 conjugation enzymes in HEK293T cells resulted in nearly complete loss of ISG15 conjugates, whereas

expression of the active-site C-to-A variant of PLpro (PLpro^{C-A}) did not. Addition of 6-TG resulted in a dose-dependent inhibition of PLpro de-ISGylation activity, with half-maximal inhibition at approximately 0.1 μM (quantitation shown in Figure S2C). To demonstrate that 6-TG acts directly on PLpro, an *in vitro* cleavage assay was established based on an ISG15 fusion protein. Like most ubiquitin-like proteins, ISG15 is synthesized in cells as a precursor protein with a C-terminal extension that must be proteolytically removed prior to conjugation. We expressed and purified the precursor form of ISG15 with an additional C-terminal HA tag (Pro-ISG15-HA), and this was used as a substrate for the purified PLpro domain (nsp3 residues 746-1061). As shown in Figure 3B, purified PLpro proteolytically removed the HA-tagged C-terminal extension, and increasing amounts of 6-TG inhibited the reaction, dependent on the input amount of PLpro enzyme (quantitation shown in Figure S2D). These results indicate that 6-TG directly inhibits SARS-CoV-2 PLpro.

DISCUSSION

The results shown here indicate that 6-TG is a direct-acting SARS-CoV-2 antiviral that functions by inhibiting the PLpro activity of the nsp3 protein. 6-TG inhibited both pp1a polyprotein processing in cells and the ISG15 deconjugation activity of PLpro in cells and *in vitro*. Pp1a polyprotein cleavage is essential for generation of the nsp1-4 viral proteins, and therefore essential for virus replication. Inhibition of ISG15 conjugation is likely to have a less important effect in cell-based replication assays but may have important consequences during an infection in an animal or human host. The fact that MERS-CoV and SARS-CoV-1 PLpro also have de-ISGylase activity suggests these viruses are particularly sensitive to the antiviral effects of ISG15. Although the critical targets of ISG15 conjugation in infected cells are not yet known, we speculate that these may include newly translated viral proteins, as suggested earlier (Durfee et al., 2010), and perhaps the pp1a protein, itself.

6-TG is an orally-delivered generic drug on the World Health Organization list of essential medicines, suggesting that it could be potentially re-purposed as an inexpensive and widely available therapeutic for COVID-19. Clinical trials are essential for determining the effectiveness of 6-TG against COVID-19. Four clinically approved hepatitis C protease inhibitors (Semeprevir, Paritaprevir, Vaniprevir, and Grazoprevir) have also recently been shown to inhibit SARS-CoV-2 PLpro *in vitro* and virus replication in Vero-E6 cells (Bafna et al., 2021). The EC50s for inhibition of viral replication for these drugs ranged from 4.25 to 10.8 μM, while that of 6-TG was determined here to be 2.13 μM. Although 6-TG directly inhibited PLpro activity, it should be noted that the mechanism of action of 6-TG as a chemotherapeutic and immunosuppressant is that it is converted into 6-Thioguanine ribonucleotides and deoxynucleotides and incorporated into RNA and DNA. It is therefore possible that incorporation of 6-TG-containing ribonucleotides into SARS-CoV-2 RNA could be a secondary antiviral effect of 6-TG.

Current 6-TG dosing in patients varies significantly, from 0.3 mg/kg/day for long-term treatment of inflammatory diseases, to up to 3 mg/kg/day in acute lymphocytic and myelogenous leukemia treatments (Seinen et al., 2010). Hepatotoxicity and bone marrow suppression are significant side effects of high dose treatment (2-3 mg/kg/day); however, this is typically not seen before two courses of treatment (2 months). 6-TG as an IBD therapeutic involves continuous doses of 0.3 mg/kg/day for more than a year, a dosage that results in fewer cases of liver and myeloid toxicities (Meijer et al., 2016; Mulder et al., 2014). Although it may seem counterintuitive to use a immunosuppressive as an antiviral, evidence to date indicates that IBD patients on thiopurine therapies do not have higher rates of COVID-19 than the general population (Higgins et al., 2020). Further, as a potential COVID-19 treatment, we anticipate that 6-TG treatment courses would be on the order of 5–10 days, like Remdesivir, and therefore toxicities and immune-suppression associated with prolonged or high dose 6-TG treatment are unlikely to be relevant. Also like Remdesivir, we anticipate that 6-TG would be most effective if administered early in the course of a SARS-CoV-2 infection, during the peak viral replication phase. We note that unlike 6-TG, Remdesivir must be delivered intravenously. We propose that the results presented here warrant the initiation of human clinical trials of 6-TG as a SARS-CoV-2 therapeutic. As PLpro is a conserved and essential enzymatic activity of the beta coronaviruses, 6-TG may prove useful in the current and future coronavirus pandemics and as a complement to other antivirals in use and in development.

Limitations of study

SARS-CoV-2 plaque assays were performed only in African Green Monkey Vero-E6 cells, and it is possible that replication assays in human cells, such as Calu3 or normal human airway epithelial cells would have

given different IC50 values that would be more relevant in considering possible human clinical trials. An additional limitation of the study is that the effects of 6-TG were not tested in a whole animal model of SARS-CoV-2 infection. Human clinical trials will ultimately be necessary to determine the effectiveness of 6-TG as a COVID-19 therapeutic.

STAR★METHODS

Detailed methods are provided in the online version of this paper and include the following:

- KEY RESOURCES TABLE
- RESOURCE AVAILABILITY
  - Lead contact
  - Material availability
  - Data and code availability
- EXPERIMENTAL MODEL AND SUBJECT DETAILS
  - Cells, viruses, and compounds
  - Plasmids
- METHOD DETAILS
  - Transfections and drug treatments
  - Protein purification
  - Pro-ISG15-HA cleavage assay
  - Immunoblotting and immunoprecipitations
  - Virus replication and plaque assays
  - Cytotoxicity assays
- QUANTIFICATION AND STATISTICAL ANALYSIS

SUPPLEMENTAL INFORMATION

Supplemental information can be found online at https://doi.org/10.1016/j.isci.2021.103213.

ACKNOWLEDGMENTS

We thank Robert Krug and Sylvie Beaudenon-Huibregtse for critical reading of the manuscript and Bill Matsui for helpful discussions. This work was supported by grants from the National Institutes of Health, National Institute of Allergy and Infectious Diseases to J. M. H. (AI096090) and D. J. L. (AI080672), a CTSA from the National Institutes of Health (UL1 TR002345) to D. J. L., and support from the College of Natural Sciences, University of Texas at Austin.

AUTHOR CONTRIBUTIONS

Conceptualization and methodology: J. M. H., D. J. L., C. D. S., Y.-C. P., L. A. C., V. K.; Investigation and data analysis: C. D. S., V. D., Y.-C. P., X. Z., H. H. H., T. L. D.; Supervision: J. M. H., D. J. L., A. C. M. B., V. K.; Writing, original draft: J. M. H.; Writing, editing: J. M. H., D. J. L., A. C. M. B., C. D. S., Y.-C. P., L. A. C.; Project administration and funding acquisition: J. M. H., D. J. L., A. C. M B, V. K.

DECLARATION OF INTERESTS

Authors declare no competing interests.

Received: June 28, 2021
Revised: September 15, 2021
Accepted: September 29, 2021
Published: October 22, 2021

REFERENCES

Bafna, K., White, K., Harish, B., Rosales, R., Ramelot, T.A., Acton, T.B., Moreno, E., Kehrer, T., Miorin, L., Royer, C.A., et al. (2021). Hepatitis C virus drugs that inhibit SARS-CoV-2 papain-like protease synergize with remdesivir to suppress viral replication in cell culture. Cell Rep. *35*, 109133. https://doi.org/10.1016/j.celrep.2021.109133.

Bayoumy, A.B., Simsek, M., Seinen, M.L., Mulder, C.J.J., Ansari, A., Peters, G.J., and De Boer, N.K. (2020). The continuous rediscovery and the benefit-risk ratio of thioguanine, a comprehensive review. Expert Opin. Drug Metab. Toxicol. *16*, 111–123. https://doi.org/10.1080/17425255.2020.1719996.

Cheng, K.-W., Cheng, S.-C., Chen, W.-Y., Lin, M.-H., Chuang, S.-J., Cheng, I.-H., Sun, C.-Y., and Chou, C.-Y. (2015). Thiopurine analogs and mycophenolic acid synergistically inhibit the papain-like protease of Middle East respiratory syndrome coronavirus. Antivir. Res. *115*, 9–16. https://doi.org/10.1016/j.antiviral.2014.12.011.

Chou, C.-Y., Chien, C.-H., Han, Y.-S., Prebanda, M.T., Hsieh, H.-P., Turk, B., Chang, G.-G., and Chen, X. (2008). Thiopurine analogues inhibit papain-like protease of severe acute respiratory syndrome coronavirus. Biochem. Pharmacol. *75*, 1601–1609. https://doi.org/10.1016/j.bcp.2008.01.005.

Coronaviridae Study Group of the International Committee on Taxonomy of Viruses (2020). The species Severe acute respiratory syndrome-related coronavirus: classifying 2019-nCoV and naming it SARS-CoV-2. Nat. Microbiol. *5*, 536–544. https://doi.org/10.1038/s41564-020-0695-z.

Daczkowski, C.M., Goodwin, O.Y., Dzimianski, J.V., Farhat, J.J., and Pegan, S.D. (2017). Structurally guided removal of DeISGylase biochemical activity from papain-like protease originating from Middle East respiratory syndrome coronavirus. J. Virol. *91*. https://doi.org/10.1128/JVI.01067-17.

Dastur, A., Beaudenon, S., Kelley, M., Krug, R.M., and Huibregtse, J.M. (2006). Herc5, an interferon-induced HECT E3 enzyme, is required for conjugation of ISG15 in human cells. J. Biol. Chem. *281*, 4334–4338. https://doi.org/10.1074/jbc.M512830200.

Durfee, L.A., Kelley, M.L., and Huibregtse, J.M. (2008). The basis for selective E1-E2 interactions in the ISG15 conjugation system. J Biol Chem *283*, 23895–23902. https://doi.org/10.1074/jbc.M804069200.

Durfee, L.A., Lyon, N., Seo, K., and Huibregtse, J.M. (2010). The ISG15 conjugation system broadly targets newly synthesized proteins: implications for the antiviral function of ISG15. Mol. Cell *38*, 722–732. https://doi.org/10.1016/j.molcel.2010.05.002.

Freitas, B.T., Durie, I.A., Murray, J., Longo, J.E., Miller, H.C., Crich, D., Hogan, R.J., Tripp, R.A., and Pegan, S.D. (2020). Characterization and noncovalent inhibition of the deubiquitinase and deISGylase activity of SARS-CoV-2 papain-like protease. ACS Infect. Dis. https://doi.org/10.1021/acsinfecdis.0c00168.

Gralinski, L.E., and Menachery, V.D. (2020). Return of the coronavirus: 2019-nCoV. Viruses *12*. https://doi.org/10.3390/v12020135.

Guy, R.K., DiPaola, R.S., Romanelli, F., and Dutch, R.E. (2020). Rapid repurposing of drugs for COVID-19. Science *368*, 829–830. https://doi.org/10.1126/science.abb9332.

Harcourt, B.H., Jukneliene, D., Kanjanahaluethai, A., Bechill, J., Severson, K.M., Smith, C.M., Rota, P.A., and Baker, S.C. (2004). Identification of severe acute respiratory syndrome coronavirus replicase products and characterization of papain-like protease activity. J. Virol. *78*, 13600–13612. https://doi.org/10.1128/JVI.78.24.13600-13612.2004.

Higgins, P.D.R., Ng, S., Danese, S., and Rao, K. (2020). The risk of SARS-CoV-2 in immunosuppressed IBD patients. Crohns Colitis 360 *2*. https://doi.org/10.1093/crocol/otaa026.

Klemm, T., Ebert, G., Calleja, D.J., Allison, C.C., Richardson, L.W., Bernardini, J.P., Lu, B.G., Kuchel, N.W., Grohmann, C., Shibata, Y., et al. (2020). Mechanism and inhibition of the papain-like protease, PLpro, of SARS-CoV-2. EMBO J. e106275. https://doi.org/10.15252/embj.2020106275.

Meijer, B., Mulder, C.J., Peters, G.J., van Bodegraven, A.A., and de Boer, N.K. (2016). Efficacy of thioguanine treatment in inflammatory bowel disease: a systematic review. World J. Gastroenterol. *22*, 9012–9021. https://doi.org/10.3748/wjg.v22.i40.9012.

Mulder, C.J.J., van Asseldonk, D.P., and de Boer, N.K.H. (2014). Drug Rediscovery to Prevent O-Label Prescription Reduces Health Care Costs: the Case of Tioguanine in e Netherlands. J. Gastrointest. Liver Dis. *23*, 123–125. https://doi.org/10.15403/jgld.2014.1121.cjjm1.

Seinen, M.L., van Asseldonk, D.P., Mulder, C.J.J., and de Boer, N.K.H. (2010). Dosing 6-thioguanine in inflammatory bowel disease: expert-based guidelines for daily practice. J. Gastrointest. Liver Dis. *19*, 291–294.

Shin, D., Mukherjee, R., Grewe, D., Bojkova, D., Baek, K., Bhattacharya, A., Schulz, L., Widera, M., Mehdipour, A.R., Tascher, G., et al. (2020). Papain-like protease regulates SARS-CoV-2 viral spread and innate immunity. Nature. https://doi.org/10.1038/s41586-020-2601-5.

Swaim, C.D., Canadeo, L.A., Monte, K.J., Khanna, S., Lenschow, D.J., and Huibregtse, J.M. (2020). Modulation of extracellular ISG15 signaling by pathogens and viral effector proteins. Cell Rep. *31*, 107772. https://doi.org/10.1016/j.celrep.2020.107772.

Swaim, C.D., Scott, A.F., Canadeo, L.A., and Huibregtse, J.M. (2017). Extracellular ISG15 signals cytokine secretion through the LFA-1 integrin receptor. Mol Cell *68*, 581–590. https://doi.org/10.1016/j.molcel.2017.10.003.

Tay, M.Z., Poh, C.M., Rénia, L., MacAry, P.A., and Ng, L.F.P. (2020). The trinity of COVID-19: immunity, inflammation and intervention. Nat. Rev. Immunol. https://doi.org/10.1038/s41577-020-0311-8.

V'kovski, P., Kratzel, A., Steiner, S., Stalder, H., and Thiel, V. (2021). Coronavirus biology and replication: implications for SARS-CoV-2. Nat. Rev. Microbiol. *19*, 155–170. https://doi.org/10.1038/s41579-020-00468-6.

Yin, W., Mao, C., Luan, X., Shen, D.-D., Shen, Q., Su, H., Wang, X., Zhou, F., Zhao, W., Gao, M., et al. (2020). Structural basis for inhibition of the RNA-dependent RNA polymerase from SARS-CoV-2 by remdesivir. Science *368*, 1499–1504. https://doi.org/10.1126/science.abc1560.

STAR★METHODS

KEY RESOURCES TABLE

REAGENT or RESOURCE	SOURCE	IDENTIFIER
Antibodies		
M2 Flag	Sigma	RRID: AB_259529
Anti-ISG15	Invitrogen	RRID: AB_2784562
Anti-Protein A	Sigma	RRID: AB_261038
Anti-NP SARS-CoV-1/SARS-CoV-2, 1C7C7	Thermo Scientific	RRID: AB_2533325
Anti-Actin	Thermo Scientific	RRID: AB_2536382
Bacterial and virus strains		
BL21 GST-SARS-CoV-2 PL^{pro}	This paper	
BL21 GST Pro-ISG15-HA	This paper	
2019 n-CoV/USA_WA1/2020	CDC	CDC/BEI Resources NR52281
Chemicals, peptides, and recombinant proteins		
PreScission Protease	GE Healthcare	CAT#27-0843-01
CellTiter-Glo 2	Promega	CAT#G9241
6-Thiogunaine	TCI	CAT#T0212
GLR0617	MCE	CAT#HY-117043
Remdesivir	APEXBIO	CAT#B8398
Azathioprine	TCI	CAT#A2069
Isopropyl β-D-1-thiogalactopyranoside	FisherSci	CAT#BP1755-10
Vectastain ABC HRP	Vector Labs	CAT#PK-4000
X-treamGENE HP DNA transfection reagent	Sigma	CAT#6366546001
Experimental models: Cell lines		
Vero E6 cells	ATCC	CAT#CRL-1586
HEK293T cells	ATCC	CAT#CRL-3216
Recombinant DNA		
pcDNA3 UBE1L	(Durfee et al., 2008)	
pcDNA3 UBCH8	(Durfee et al., 2008)	
pcDNA3 HA HERC5	(Durfee et al., 2008)	
pcDNA3 3xFLAG-WT ISG15	(Swaim et al., 2017)	
pGEX-6p SARS-CoV-2 PL^{pro}	This paper	
pcDNA TAP-$NSP123^{WT}$	This paper	
pcDNA TAP-NSP123 C1675A	This paper	
pcDNA NTAP SARS-CoV-2 PL^{pro}	Swaim et al., 2020	
pcDNA NTAP SARS-CoV-2 PL^{pro} C110A	Swaim et al., 2020	
Software and algorithms		
Prism 8	Graphpad	
Other		
BOLT Bis Tris 4-12% gel	Thermo Scientific	CAT#NW04120BOX
Sera mag speed bead protein AG	GE lifesciences	
NuPAGE Tris Acetate 3-8% gel	Thermo Scientific	CAT#EA0375PK2
Protein A sepharose	Invitrogen	CAT#101141
Glutathione Sepharose	GE Healthcare	CAT#17075601

RESOURCE AVAILABILITY

Lead contact

Further information and requests for resources and reagents should be directed to and will be fulfilled by the lead contact, Jon Huibregtse (huibregtse@austin.utexas.edu).

Material availability

All newly generated reagents for this study are available at the institution of the lead contact.

Data and code availability

Not applicable.

EXPERIMENTAL MODEL AND SUBJECT DETAILS

Cells, viruses, and compounds

All cell lines were maintained at 37°C, 5% v/v CO_2 in a humidified incubator. HEK293T cells were grown in DMEM (Corning) supplemented with 10% FBS (Sigma) and 1% Penicillin-Streptomycin (Corning). Vero-E6 (ATCC), were cultured at 37°C, 5% v/v CO_2 in a humidified incubator in Dulbecco's Modified Eagle medium (Corning) supplemented with 10% FBS (HyClone), 1% Penicillin-Streptomycin (Corning), 10 mM HEPES (Corning), and 1X non-essential amino acids (Sigma). Infections and culture post infection was conducted in DMEM with 2% FBS, 1% Penicillin-Streptomycin, 10mM HEPES, and 1X non-essential amino acids.

SARS-CoV-2, USA-WA1/2020 strain (Genbank: MN985325.1), was obtained from The Biological and Emerging Infections Resources Program (BEI Resources NR-52281). A 6th passage (P6) of SARS-CoV-2 was generated by infecting Vero-E6 cells obtained from ATCC (CRL-1586) for 72 hours (h). At 72 h post infection, culture supernatants were collected, clarified, and aliquots were stored at -80°C. Viral titers were calculated by conventional plaque assay.

Plasmids

pcDNA3.1-TAP-PLpro^{WT} and pcDNA3.1-TAP-PLpro^{CA} were described in Swaim et al. (2020). pcDNA3.1-TAP-nsp123 was generated from a partial orf1ab clone (S2-A2_p57 plasmids) encoding residues 1-1504; nsp1, nsp2, and part of nsp3; (gift from Hongbing Jiang and David Wang, Washington University School of Medicine) with the remainder of the nsp3 ORF (residues 1505 - 2767 of pp1a, derived from Addgene cat# 141257). The pcDNA3.1-TAP-nsp123 active site variant (C to A substitution, residue 1675 of polyprotein 1a, corresponding to residue 856 of mature nsp3) was generated from this clone by overlapping PCR. Plasmids expressing FLAG-ISG15, and the ISG15 E1, E2, and E3 enzymes (Uba7, Ube2L6, and Herc5) have been described previously (Swaim et al., 2017). Pro-ISG15-HA was generated by appending the natural C-terminal ISG15 extension and an HA-tag (GTEPGGRSYPYDVPDYA) to the C-terminus of FLAG-ISG15. The TAP-nsp2-3 was generated by amplifying the region encoding the last 92 amino acids of nsp2 and the first 100 amino acids of nsp3 (residues 727-918 of pp1a) from TAP-nsp123 and cloning it into pcDNA-NTAP using the BamH1 and Not1 restriction sites.

METHOD DETAILS

Transfections and drug treatments

HEK293T cells were plated in a 6 well plate at a density of $3x10^4$ cells/mL. The next day cells were transfected using X-tremeGENE HP DNA transfection reagent (Roche). Plasmids were transfected at the following amounts: 0.35 μg FLAG-ISG15, 0.25 μg Uba7, 0.25 μg Ube2L6, 0.35 μg HA-Herc5, 1 μg TAP-nsp123 (WT or CA), 0.2 μg TAP-PLpro (WT or CA) Cells were treated with 6-TG at the indicated concentrations immediately following transfection (100 mM 6-TG stock in DMSO and diluted in PBS).

Protein purification

Sars-CoV-2 PLpro was purified as a GST fusion protein in BL12 *E. coli*. Overnight starter cultures were grown at 37°C for 16 hours. Cultures were diluted 1:10 and cultured with shaking for 2 hours at 37°C. Expression of protein was induced with 100 μM Isopropyl β-D-1-thiogalactopyranoside (IPTG) for 24 hours at 16°C. Cells were collected by centrifugation, resuspended in 10 mL TBS with 0.00025% Tween 20, 0.01 mM DTT and 5% glycerol (Binding Buffer), and sonicated for 1 minute. Lysates were spun at 15,000 x g for 10 minutes and supernatants were incubated with 100 μL per liter of culture Glutathione Sepharose (GE Healthcare) for

4 hours with rotation at 4°C. Beads were collected and washed three times with Binding Buffer supplemented with 0.1mM EDTA and subjected to site-specific cleavage with PreScission Protease (GE Healthcare) to remove the GST tag. Beads were removed and the protein concentration in the supernatant was quantified by SDS-PAGE using a Licor Odyssey Imager.

Pro-ISG15-HA was purified as a GST fusion from BL21 E. coli. Overnight starter cultures were grown at 37°C. Cultures were diluted 1:10 with shaking for 2 hrs at 37°C. Expression of protein was induced with 100 μM Isopropyl β-D-1-thiogalactopyranoside (IPTG) for 3 hours at 30°C. Cells were collected by centrifugation and resuspended in PBS with 1% Triton X and sonicated for 30 seconds. Lysates were spun at 15,000 x g for 10 minutes and supernatants were incubated with 100 μL per liter of culture Glutathione Sepharose (GE Healthcare) for 4 hours with rotation at 4°C. Beads were collected and washed three times with Binding Buffer supplemented with 0.1mM EDTA and subjected to site-specific cleavage with PreScission Protease (GE Healthcare) to remove the GST tag. Beads were removed and the protein concentration in the supernatant was quantified by SDS-PAGE using a Licor Odyssey Imager.

Pro-ISG15-HA cleavage assay

The indicated concentrations of PLpro were incubated with increasing concentrations of 6-TG for 1 min at a 40 μL volume. 100 ng (166 nM) of Pro-ISG15-HA was added to the PLpro-6-TG reactions for 30 min. The reactions were stopped with the addition of 10μL of loading buffer (25mM Tris pH6.8 40% glycerol, 8% SDS and 4mM DTT) and analyzed by HA-immunoblot; loss of the HA tag reflects proteolytic cleavage by PLpro.

Immunoblotting and immunoprecipitations

Samples assessing ISGylation were lysed in 1% NP40 lysis buffer (100 mM Tris pH 7.5, 100 mM NaCl ,1% NP40) supplemented with 10 mM NEM, 170 μg/mL PMSF, 2 μg/mL leupeptin, 2 μg/mL aprotinin and 10 mM DTT for 10 minutes on ice followed by a 10 minute spin at 20,000 x *g*. Samples were run on BOLT 4-12% Bis-Tris gels (Thermo) and blotted with anti-M2 FLAG antibody (Sigma) and anti-actin (Invitrogen AC-15). Samples assessing the effect of 6-TG on TAP-nsp123 cleavage were lysed in RIPA buffer (50 mM Tris pH 8, 150 mM NaCl, 0.5% NP40, 0.1% SDS, 0.5% Sodium deoxycholate w/v) supplemented with 10 mM NEM, 170 μg/mL PMSF, 2 μg/mL leupeptin, 2 μg/mL aprotinin, 10 mM DTT, and 2 units/mL Universal Nuclease (Pierce) and incubated for 10 minutes on ice followed by a 10 minute spin at 20,000 x *g*. Samples were run on 3-8% Tris-Acetate gels (Thermo) and blotted for TAP using anti-protein A antibody (Sigma) and anti-actin (Invitrogen AC-15).

Virus replication and plaque assays

Vero-E6 cells (2 x 10^4 cells/well) were seeded in 96-well culture plates in DMEM +10% FBS+P/S/G and incubated at 37°C, 5% CO2. After 24 h, Vero-E6 cells were infected with SARS-CoV-2 (MOI 0.01; 50 μl) for 1 h at 37°C; 5% CO2. After 1 h of viral adsorption, virus inoculum was removed and post-infection media (DMEM + 2% FBS + P/S/G) containing ten-fold serially diluted 6-TG, GLR0617, and Azathioprine (100 μM to 0.1 pM) with 1% Avicel was added. Remdesivir was diluted 3-fold (100 μM-0.01 μM) and served as a positive control. Cells infected with SARS-CoV-2 only, cells alone (mock infected cells), and DMSO, were included as controls. At 24 h post-infection, the overlay media was removed and plates were fixed overnight in 10% neutral buffered formalin (Sigma-Aldrich), followed by 3 washes with PBS. Cells were stained with SARS-CoV nucleocapsid (N) protein cross-reactive monoclonal antibody (mAb, 1C7C7, Cat# ZMS1075, Sigma-Aldrich, Saint Louis, MO) diluted in 1% Bovine Serum Albumin (BSA,1 μg/ml) for 1 h at 37°C and washed with PBS. 150 μL of biotinylated secondary antibody was added (Vector Laboratories PK-4000) for 30 min at 37°C with 5% CO2. Post secondary antibody incubation the ABC reagent was added for 30 min at room temperature (Vector Laboratories PK-4000). Plates were washed 3 times with PBS and developed using DAB staining (Vector Laboratories SK-4100) per manufacturer's instructions. The plates were scanned using a CTL ImmunoSpot plate reader, and formed plaques were counted by an automated counting software (Cellular Technology Limited, Cleveland, OH, USA). Plaque forming units were calculated relative to DMSO treated controls.

Cytotoxicity assays

CellTiter-Glo 2.0 (Promega) was used to determine the cytotoxicity of Remdesivir, 6-TG, GLR0617, and Azathioprine. Vero-E6 cells were seeded in a 96 well white clear bottom plate at 2.5x10^5 cells per well in

100 μL of media for 16 hours. Compounds including a DMSO control were added at the indicated concentrations for 48 hours in triplicate. After 48 hours the plate was brought to room temperature and 100μL of CellTiter-Glo 2.0 was added to each well. The plate was placed on an orbital shaker for 2 minutes and then incubated in the dark for 10 minutes. The plate was read on a spectromax M3 plate reader luminometer with an integration time of .5 seconds per well. Luminescence of compound treated samples was compared to no-cell background and to DMSO treated cells to determine percent survival, and plotted using Graphpad Prism 9. Non linear fit vs. normalized response with variable slope was used to calculate CC50 values for each compound.

QUANTIFICATION AND STATISTICAL ANALYSIS

Graphpad Prism 9 software was used to plot virus replication and densitometry data. Bars represent three or more biological replicates. Error bars represent the standard error of the mean (SEM). Ordinary one-way ANOVA was performed on each data set. A non-linear regression curve fit analysis over the dilution curve was performed to calculate EC50 and CC50 of the compounds. Cell viability, dose response curve, and EC50 with 95% confidence intervals are indicated on the graph (Figure S2).